



ELSEVIER

Surgery for Obesity and Related Diseases ■ (2014) 00–00

SURGERY FOR OBESITY
AND RELATED DISEASES

Original article

Expression of tight-junction proteins in human proximal small intestinal mucosa before and after Roux-en-Y gastric bypass surgery

Anna Casselbrant, Ph.D., M.Sc.^{*}, Erik Elias, M.D., Lars Fändriks, Ph.D., M.D.,
Ville Wallenius, Ph.D., M.D.

Department of Gastrointestinal Research and Education, Institute of Clinical Sciences, Sahlgrenska Academy, University of Gothenburg, Sweden

Received January 27, 2014; accepted May 5, 2014

Abstract

Background: Increased permeability and uptake of proinflammatory bacterial endotoxins from gut microbiota has been suggested as a mechanism for obesity-associated chronic inflammation that causes obesity-associated insulin resistance. We hypothesized that intestinal barrier function may be restored after Roux-en-Y gastric bypass (RYGB) surgery and thereby contribute to decreased inflammation. The objective of this study was to investigate levels of the permeability-regulating tight-junction proteins in human small intestinal mucosa before and after RYGB surgery.

Methods: Paired intraindividual jejunal mucosa samples were retrieved at the time of surgery and 6 to 8 months after surgery. Mucosal cell surface area was calculated by histomorphometry. Mucosal samples were analyzed by proteomics to find patterns of protein regulations. Based on these findings further analyses were performed by Western blotting. Ussing chambers were used to analyze permeability in the retrieved mucosal samples.

Results: Mucosal surface area was significantly decreased after surgery. Global protein expression analysis showed a significant increase in the cytokeratin-8 (Ck8), which was confirmed by Western blotting. Further analyses showed a significant increase in claudin-3 and -4 expression after surgery, whereas occludin and zonula occludens-1 levels were decreased. Expressions of claudin-1, -2, -5 and vinculin were unchanged. Ussing chamber experiments revealed a linear correlation between the epithelial electrical resistance and claudin-3 protein expression.

Conclusion: Several alterations were found in the rerouted small intestine after surgery, indicating a decreased jejunal mucosal surface area and decreased paracellular permeability. These changes could contribute to decreased uptake of luminal microbiota-derived inflammatory mediators such as endotoxins after RYGB. (Surg Obes Relat Dis 2014;■:00–00.) © 2014 American Society for Metabolic and Bariatric Surgery. All rights reserved.

Keywords:

Small intestine; Epithelial resistance; Tight junction; Obesity; Roux-en-Y gastric bypass

In the last decade, accumulating evidence has provided new insights regarding the influence of the gut microbiota and its interactions with the host immunity and metabolism in the most prevalent metabolic disease, obesity [1]. By several mechanisms the gut microbiota seem to influence

the chronic low-grade inflammation that accompanies obesity, and may even contribute to the increased fat deposition itself that eventually leads to insulin resistance and type 2 diabetes [2,3]. Endotoxins, e.g., lipopolysaccharide (LPS), that are major components of the bacterial outer cell membrane, have been identified as triggering and inflammatory factors causative of an intestine-derived inflammatory response in animal models of obesity, e.g., contributing to the onset of nonalcoholic steatohepatitis [4,5]. The large amounts of LPS in the intestinal microflora

^{*}Correspondence: Anna Casselbrant, Ph.D., M.Sc., Dept. of Gastrointestinal Research and Education, Instit. of Clinical Sciences, Sahlgrenska Academy, University of Gothenburg, Bruna stråket 20, SE413 45 Gothenburg, Sweden.

E-mail: anna.casselbrant@gastro.gu.se

are the major source for circulating endotoxins that are considered key events in the development of the chronic low-grade inflammatory state found in obese individuals [6]. Interestingly, studies have shown that the proportion of LPS in the microflora is higher in obese patients than in lean patients [7,8]. Furthermore, studies have shown that high-fat diet increased plasma levels of LPS and inflammation in comparison with a control diet [9], and that there was a positive correlation between intake of high energy diets and endotoxemia [2,10].

Intestinal permeability is related to the properties of the membrane that allow molecules to cross from the lumen. Absorption and secretion take place either through cells (transcellular) or between cells (paracellular). The paracellular transport capacity is dependent on the mechanical linkage between epithelial cells: the apical junction structures and the tight junctions (TJs). The movement of substances across paracellular space is under influence of several factors such as the concentration gradient across the barrier, the surface area of the epithelium, the time available for diffusion, and the intrinsic permeability properties of the barrier itself. Three main factors have been suggested to influence intestinal permeability: the host-microbe interactions of the intestinal tract [11], the dietary pattern [12], and nutritional deficiencies [13].

Bariatric surgery is currently the most effective treatment of obesity and its co-morbidities. Roux-en-Y gastric bypass (RYGB) surgery results in a substantial and long-term weight loss as well as resolution of type 2 diabetes [14]. Furthermore, RYGB has a powerful effect in preventing development of type 2 diabetes in obese patients [15]. RYGB also leads to a decrease of the chronic state of inflammation that is seen in obesity [16]. After RYGB surgery, patients also display major changes in eating behavior and dietary intake [17], as well as food preference [18]. Changes in dietary selection, in for example fat intake, may be important for the intestinal barrier function [9,18]. Therefore, we hypothesized that improved mucosal tight junction function in the proximal small intestine may contribute to normalized barrier function after RYGB. It

could thereby eventually contribute to decreased gut-derived inflammation and lead to improvement in obesity-associated metabolic complications such as type 2 diabetes and cardiovascular disease. To our knowledge, there are no reports on the effects of RYGB surgery in humans on the expression of TJ proteins in small intestinal mucosa. The aim of the present study was to investigate the expression levels of TJ proteins in human small intestinal mucosa before and after RYGB surgery. Intestinal permeability was measured by the Ussing chamber technique.

Methods

Patients

Jejunal tissues of full wall thickness were obtained from 33 patients undergoing a first time laparoscopic RYGB or a conversion from vertical banded gastroplasty to RYGB (Table 1) at Sahlgrenska University Hospital, Gothenburg, Sweden. The operative technique included an antecolic-antegastric Roux-en-Y construction with a 10–20 mL gastric pouch. The gastroenteroanastomosis was constructed using a straight 45-mm stapler and complementary hand suturing thus creating a wide open gastroenteroanastomosis. The length of the pancreatobiliary limb was 50–60 cm from the ligament of Treitz. A full-wall specimen was resected from the jejunum between the gastroentero and the entero-entero anastomosis as the bowel loop was divided to create the Roux-en-Y construction as earlier described [19]. After excision, the mucosal/submucosal biopsy was retrieved by using an endoscopic biopsy forceps, to make sampling depth as similar as possible to the postoperative sampling by gastroscopy. Tissue specimens were taken for proteomics and western blot analyses, histomorphometry and Ussing chamber experiments as described below. The study was approved by the Ethics committee of Gothenburg University and by the Regional Ethical Review Board in Gothenburg and was performed in accordance with the Declaration of Helsinki. All patients signed an informed consent form before inclusion into the study.

Table 1
Clinical data

Preoperative data	Total (n = 33)	Male (n = 7)	Female (n = 26)
Age (yr)	48.9 (68–25)	51.3 (67–39)	48.3 (68–25)
BMI (kg/m ²)	44.1 (56.3–31.2)	42.8 (50.7–37.4)	44.4 (56.3–31.2)
Total body mass (kg)	128.2 (183–88)	146.3 (183–128)	123.1 (159–88)
Diabetes	11	3	8
Postoperative data	Total (n = 15)	Male (n = 4)	Female (n = 11)
BMI (kg/m ²)	32 (41.3–25.9)	31.9 (40.3–25.9)	32.1 (41.3–26.2)
Total body mass (kg)	90.8 (135–59)	99.6 (135–84)	88.2 (116–59)
Weight loss (%)	29.4 (10.4–43.3)	31.6 (10.4–40.2)	28.6 (15.6–43.3)
Diabetes	1	1	0
HbA1 c (mmol/mol)	37.2 (76–21)	47.3 (76–31)	35.6 (51–21)

BMI = body mass index; HbA1 c = glycated hemoglobin.

Between 6 and 8 months after surgery, 15 patients underwent an endoscopic examination of the Roux-limb, strictly for research purposes. There was no underlying disease or suspected pathology in any of these patients. Mucosal biopsies were collected approximately 8-cm distal to the stoma, thus in close proximity to where the initial tissue sample was taken.

Histomorphometry

Jejunal specimens were fixed in buffered 4% formaldehyde, dehydrated and embedded in paraffin. For evaluation, 4- μ m sections were mounted on slides and stained with hematoxylin and eosin. In coded sections of the full-thickness specimens from time of surgery and the endoscopically retrieved mucosal postsurgery biopsies were used for morphometry. The total area of the mucosal surface in relation to the relatively flat muscularis mucosae was assessed by the gridline intersection method. This method has previously been described by Mayhew [20].

Proteomics analysis

Mucosal tissue specimens from 7 patients were snap-frozen in liquid nitrogen and kept frozen (-70°C) for later analysis of protein expression. Global protein expression analysis of proximal jejunal mucosal epithelium was performed by 2-D gel electrophoresis and mass spectrometry by nanoflow Liquid chromatography-tandem mass spectrometry (LC MS/MS). In brief, biopsy samples were lyophilized and grinded to a coarse powder. Protein was dissolved in sample solubilization buffer consisting of 7 M urea, 2 M thiourea, 50 mM SDS, 50 mM 3-[(3-cholamidopropyl)dimethylammonio]-2-hydroxy -1-propanesulfonate (CHAPS), 50 mM Tris-HCl, pH 8.0. Interfering substances were removed by using the ProteoExtract Protein Precipitation Kit (Calbiochem, Darmstadt, Germany). The pellet was resolved in labelling buffer (7 M urea, 2 M thiourea, 4% CHAPS, 30 mM Tris-HCl, pH 8.5) and protein concentration was determined by the Noninterfering Protein Assay Kit (Calbiochem). All samples were diluted to a final protein concentration of 2 $\mu\text{g}/\mu\text{l}$ each. Each sample (50 μg) was labeled with 400 pmol of respective CyDye and pooled after the standard protocol (GE Healthcare, Uppsala, Sweden). Isoelectric focusing was done in 24 cm pH 3-11 Nonlinear Imobiline DryStrip (GE Healthcare) on an Ettan IPGphor. The second dimension was run on an Ettan DALT II in in-house made 1 mm acrylamide (T = 11%, C = 2.6%). Bis-Tris gel with standard 3-(N-morpholino) propanesulfonic acid (MOPS) cathode buffer and acetic acid/diethanol amine anode buffer. Gel images were analyzed using the DeCyder 2-D Differential Analysis Software v6.0 (GE Healthcare). Spots were selected for spot picking and further MS analysis. Selected protein spots, on a preparative gel of pooled samples to a total protein

concentration of 450 μg stained with SYPRO Ruby, were picked and trypsinated in the Ettan Spot-handling Workstation (GE Healthcare). The method for in-gel protein digestion with trypsin described by Shevchenko et al. [21] was applied with some minor modifications. Briefly, the gel pieces were destained by washing 3 times in 25 mM NH_4HCO_3 in 50% CH_3OH and 1 time in 70% CH_3CN . Gel pieces were dried and incubated with digestion buffer (50 mM NH_4HCO_3 , 10 ng/ μl trypsin) at 37°C for 3 hours. Peptides were extracted in 50% CH_3CN / .5% TFA and the supernatant was evaporated to dryness. Before MS analysis, the peptides were reconstituted in .2% HCOOH. Sample injections were made with an HTC-PAL autosampler (CTC Analytics AG, Zwingen, Switzerland) connected to an Agilent 1100 binary pump (Agilent Technologies, Palo Alto, CA, USA). The peptides were trapped on a precolumn (45 \times .075 mm i.d.) and separated on a reversed phase column, 200 \times .050 mm. Both columns are packed in-house with 3 μm Reprosil-Pur C_{18} -AQ particles. The flow through the analytical column was reduced by a split to approximately 100 nl/min. A 40 min gradient 10–50% CH_3CN in .2% COOH was used for separation of the peptides. The nanoflow LC-MS/MS were performed on a hybrid linear ion trap-FTICR (trap-Fourier transform ion cyclotron resonance) mass spectrometer equipped with a 7 T ICR magnet (LTQ-FT, Thermo Electron, Bremen, Germany). The spectrometer was operated in data-dependent mode, automatically switching to MS/MS mode. MS-spectra were acquired in the FTICR, while MS/MS-spectra were acquired in the LTQ-trap. For each scan of FTICR, the 3 most intense, doubly or triply charged, ions were sequentially fragmented in the linear trap by collision induced dissociation. All the tandem mass spectra were searched by MASCOT (Matrix Science, London, United Kingdom) against all species in the National Center for Biotechnology Information (NCBI) database. The search parameters were set to: MS accuracy 5 ppm, MS/MS accuracy .5 Da, 1 missed cleavage by trypsin allowed, fixed propionamide modification of cysteine and variable modification of oxidized methionine. For protein identification the minimum criteria were, 1 tryptic peptide matched. Only proteins that were regulated in the same direction in all patients ($n = 7$), and at least 50% from baseline were selected for further analysis.

Western blot analysis

Mucosal jejunal specimens were snap-frozen in liquid nitrogen and kept frozen for later Western blot analysis. The frozen specimens were sonicated in a PE buffer (10 mM potassium phosphate buffer, pH 6.8 and 1 mM ethylenediaminetetraacetic acid (EDTA)) containing 10 mM 3-[(3-cholamidopropyl) dimethylammonio]-1-propane sulphonate (CHAPS: Boehringer Mannheim, Mannheim, Germany) and the protease inhibitor cocktail tablet Complete

(Roche Diagnostics AB, Stockholm, Sweden). The homogenate was then centrifuged (10,000 g for 10 min at 4°C), and the supernatant was analyzed for protein content by the Bradford method [22]. Samples were diluted in SDS buffer and heated at 70°C for 10 min before they were loaded on a NuPage 10% Bis-Tris gel, and electrophoresis run using a MOPS or 2-(N-morpholino)ethanesulfonic acid (MES) buffer depending on the protein size (Invitrogen AB, Lidingö, Sweden). One lane of each gel was loaded with prestained molecular weight standards (SeeBlue, NOVEX, San Diego, CA, USA). After the electrophoresis the proteins were transferred to polyvinylidene difluoride membranes (Amersham, Buckinghamshire, UK), which was incubated with the following primary antibodies: Rabbit Cytokeratin (Ck)8 antibody (ab53708) and Rabbit antivinculin antibody, (ab73412; Abcam, Cambridge, UK), Rabbit anti-claudin 1 (51-9000), Rabbit anti-claudin 2, (51-6100), Rabbit anti-claudin 3 (34-1700), Mouse anti-claudin 4 (32-9400), Mouse anti-claudin 5 (35-2500), Mouse antioccludin (33-1500), Rabbit anti-ZO-1 (61-7300; Invitrogen AB, Lidingö, Sweden). An alkaline phosphatase conjugated secondary goat antimouse or goat antirabbit IgG antibody (Santa Cruz) with CDP-Star (Tropix, Bedford, MA, USA) as substrate were used to identify immunoreactive proteins by means of chemiluminescence. Images were captured by a Chemidox XRS cooled charge coupled device camera, and analyzed with Quantity One software (camera and software from BioRad laboratories, Hercules, CA, USA). Glyceraldehyde 3-phosphate dehydrogenase (GAPDH, IMG-5143 A, Imgenex, BioSite, San Diego, CA, USA) was used as control for equal loading. For each tested sample, the optical density of primary antibody divided by GAPDH represents the result. The membranes were stripped for reprobing with other primary antibodies using a stripping buffer (Re-Blot Plus Mild Solution (10 X), Millipore, Temecula, CA, USA).

Ussing chamber experiments

After receiving the tissue, it was immediately immersed in ice-cold oxygenated Krebs solution containing (in mM) 118.07 NaCl, 4.69 KCl, 2.52 CaCl₂, 1.16 MgSO₄, 1.01 NaH₂PO₄, 25 NaHCO₃ and 11.10 Glucose. The mucosa was gently dissected from the muscular layer and mounted in vertical Ussing chambers with a 4 × 8-mm oblong opening resulting in an area of .29 cm² (Warner instruments, Hamden, CT, USA). Both the luminal and the serosal sides were bathed in 5 mL Krebs solution, continuously oxygenated and stirred with 95% O₂ and 5% CO₂ gas flow at 37°C. In general, 6 Ussing chambers for jejunum were mounted per individual. Potential difference (PD) was measured with a pair of matched calomel electrodes (REF401, Radiometer analytical, Denmark) and the epithelial electrical resistance (Rep) was assessed by use of the Ussing Pulse Method. The latter has the advantage of estimating specifically Rep and is described in detail elsewhere [23]. Epithelial current (I_{ep}) is then calculated

using Ohm's Law, where I_{ep} = PD/Rep. In the present set-up data sampling and pulse inductions were computer controlled using specially constructed hardware and software developed in LabView (National Instruments, Austin, TX, USA).

Experimental procedures. After an equilibration period of 20 minutes, basal parameters were measured over 30 minutes.

Data analysis and statistics

Friedman's and Wilcoxon's signed rank test for related variables were used for analyzing the differences in protein expression. Associations between Rep and TJ protein expression were tested by Spearman's correlation. Data are presented as mean ± SEM. Individuals are denoted n and preparations/observations are denoted N. The statistical software programs SPSS 19.0 and 20.0 were used (SPSS, Chicago, IL, USA). P values of < .05 were considered significant.

Results

Jejunal histomorphometry before and after RYGB surgery

The enlargement of the luminal surface area due to the villi structure, described as the total area of the mucosal surface in relation to the relatively flat area of the muscularis mucosae, was lower in all individuals after surgery. The enlargement ratio villi/basal area was 9.08 ± .45 before (n = 9, N = 26) and 6.68 ± .64 (n = 5, N = 8) after RYGB surgery (P = .017) (Fig. 1).

Proteomics analysis of jejunal mucosa before and after RYGB surgery

Global protein expression analysis of mucosal jejunal biopsies preoperatively and 6–8 months postoperatively after RYGB surgery was performed. As mentioned, we chose a relatively conservative strategy, only analyzing proteins that were regulated in the same direction in all patients (n = 7), and at least 50% from baseline. This showed, among 27 regulated protein spots, significant changes in the signal intensities of 2 groups of proteins that were predicted to be related to the integrity of the cytoskeletal structure or to the anchoring of TJ proteins to the cytoskeleton. Eight of these protein spots were identified by mass spectroscopy as cytokeratin-8 (Ck8). These were increased 1.7–2.2 fold (mean 2.0, P < .01, n = 7). Three protein spots were identified as vinculin, and were decreased 1.7–1.8 fold (mean -1.7, n = 7, P < .05).

Western blotting of cytoskeletal and TJ proteins in jejunal mucosa

To confirm the proteomics findings, paired intraindividual jejunal mucosal samples were examined by Western blotting before and after RYGB surgery. The Ck8 protein expression changes were confirmed by Western blotting in 9 additional patients analyzed, with increased levels after

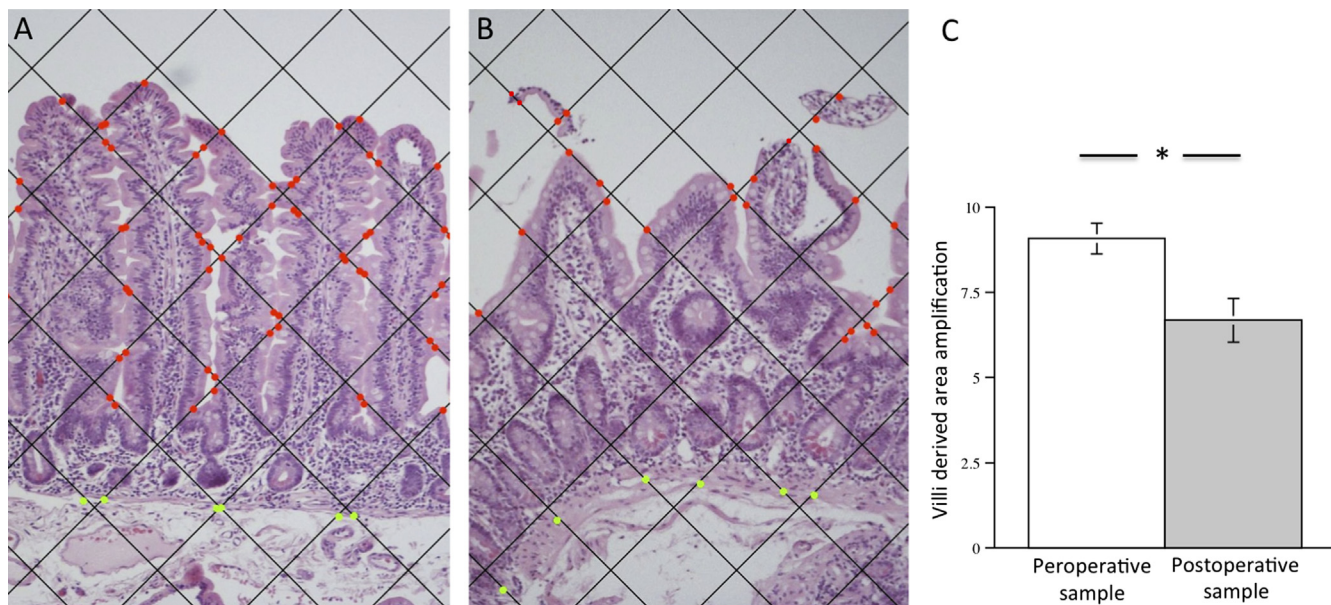


Fig. 1. Histomorphometric analysis of surface area of jejunal mucosal samples from the time of surgery and 6–8 months post-RYGB. The total area of the mucosal surface in relation to the relatively flat muscularis mucosae was assessed by the gridline intersection method; villi derived area amplification, given as hits over the mucosal surface (red dots)/hits over the muscularis mucosae (green dots). Representative hematoxylin/eosin stained sections of jejunal mucosa are shown in (A) before (enlargement factor $59/6 = 9.8$)(10 \times) and (B) after RYGB from the same individual (enlargement factor $26/6 = 4.3$)(10 \times). (C) The quantification of mucosal area in several individuals at the time of surgery (N = 26) and after (N = 8) RYGB showed a significant reduction of the surface area ($P = .017$).

surgery ($P = .017$, $n = 15$) (Fig. 2A). The decreased vinculin expression could however not be confirmed by Western blotting ($P = .314$, $n = 9$) (Fig. 2B).

We also analyzed the expressions of TJ proteins; claudins 1–5 (Fig. 3A–E), as well as occludin and zonula occludens-1 (ZO-1), by Western blotting (Fig. 3F and G). The protein expressions of claudin-3 and claudin-4 were significantly increased 6–8 months after surgery ($P = .031$ and $P = .009$, respectively, $n = 15$; Fig. 3C and D). The protein expressions of occludin and ZO-1 were however decreased after surgery ($P = .046$ and $P = .036$, respectively, $n = 9$; Fig. 3G and H), while the expression of claudins-1, 2 and 5 were unchanged (n

$= 15$) (Fig. 3A, B, and E). Grouped analysis of the TJ protein expressions in diabetics and nondiabetics before surgery showed no significant differences between the groups. Multivariate correlation analysis between the changes of TJ and Ck8 protein expressions after RYGB, versus diabetes, preoperative body mass index (BMI), and the change of BMI did not show any significant interactions between these parameters.

Electrical resistance in the jejunal mucosa

The baseline epithelial electrical parameters in the jejunal mucosa were as follows: PD $4.2 \pm .3$ mV, epithelial

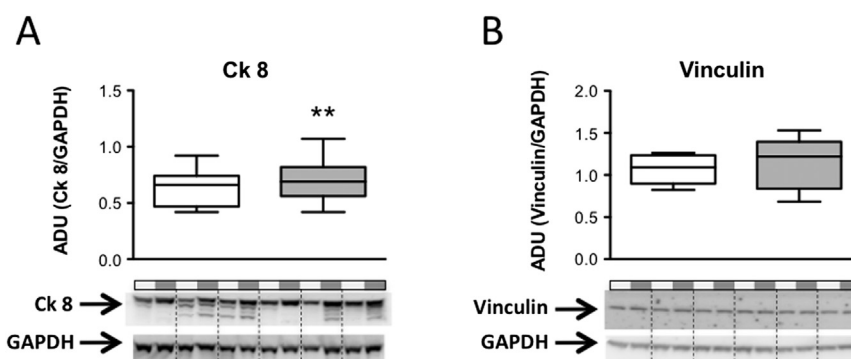


Fig. 2. Results from the Western blots showing protein expressions in paired intraindividual jejunal mucosal samples before and 6–8 months after RYGB surgery. Representative samples of protein bands of cytokeratin 8 (A) (Ck8) and vinculin (B). The box plots show medians and quartiles, whiskers show 5–95th percentiles. The protein bands for the loading control Glyceraldehyde 3-phosphate dehydrogenase (GAPDH) are also shown. The membrane is showing 6-paired individuals with typical optical density. Significant differences are indicated with asterisks (* P value for related variables using Wilcoxon's signed rank test, $n = 15$ for Ck8 and $n = 9$ for vinculin).

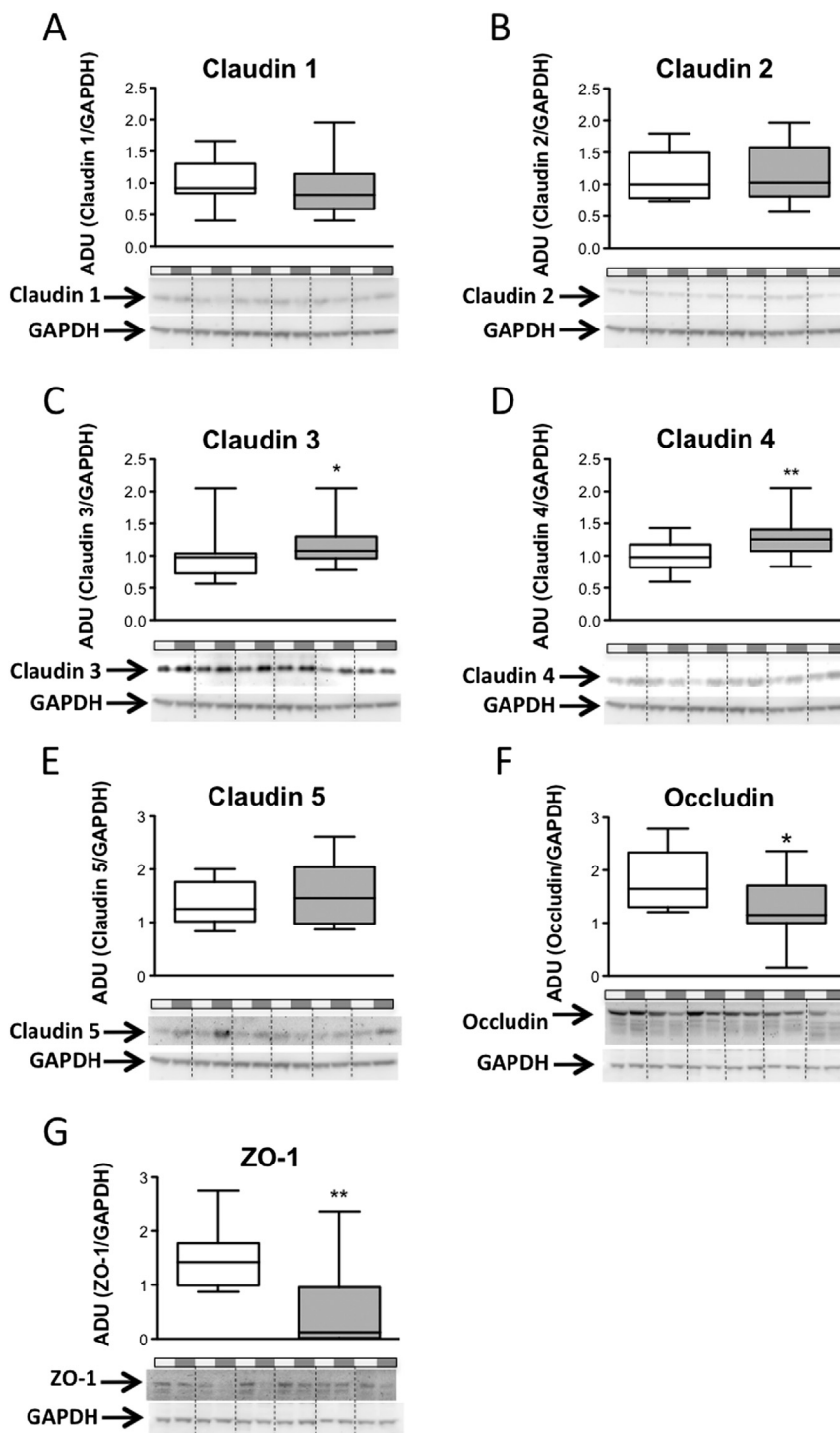


Fig. 3. Results from the Western blots showing protein expressions in paired intraindividual jejunal mucosal samples before and 6 to 8 months after RYGB surgery. Representative samples of protein bands of claudin-1 (A), claudin-2 (B), claudin-3 (C), claudin-4 (D), claudin-5 (E), occludin (F), and zonula occludens-1 (ZO-1) (G). The box plots show medians and quartiles, whiskers show 5–95th percentiles. The protein bands for the loading control Glyceraldehyde 3-phosphate dehydrogenase (GAPDH) are also shown in the figure. The membrane is showing 6-paired individuals with typical optical density. Significant differences are indicated with asterisks (**P* value for related variables using Wilcoxon's signed rank test, *n* = 15 for claudin-1, 3, 4, 5 and *n* = 9 for claudin-2, ZO-1 and occludin).

electrical resistance (*Rep*) $11.7 \pm .9 \Omega \cdot \text{cm}^2$, epithelial electrical current (*I_{ep}*) $368.8 \pm 44.7 \mu\text{A}/\text{cm}^2$ (*n* = 25, *N* = 150). Plotting data from the experiments revealed a

linear correlation between *Rep* and claudin-3 protein expression in jejunal mucosal samples that were taken during RYGB surgery from a large number of individuals (*R* = .45 and

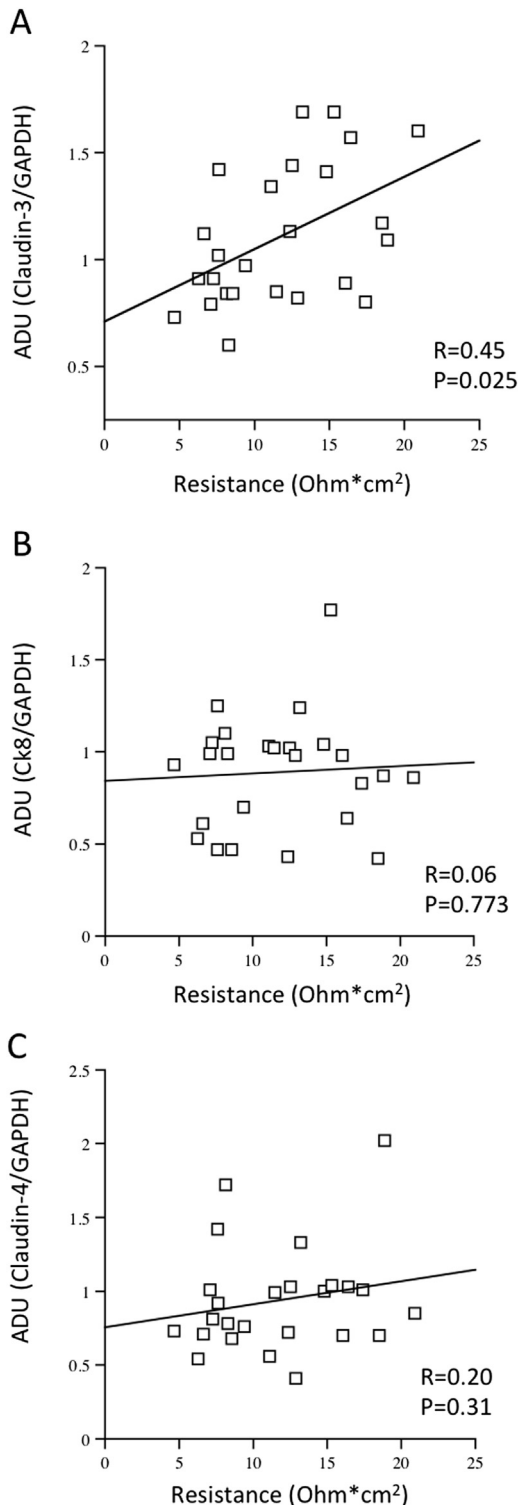


Fig. 4. Correlation analysis between tight junction protein expression and the epithelial electrical resistance in jejunal mucosa samples that were taken at the time of surgery for RYGB; (A) Claudin-3, (B) Ck8 and (C) Claudin-4 (n = 25 for all).

P = .025, n = 25, N = 150; Fig. 4A). No correlations were found between Rep and the other proteins that were increased by RYGB; Ck8 or claudin-4 (Fig. 4B and C) or

any of the other investigated TJ proteins vinculin, claudin-1, 2, 5, occludin or ZO-1 (n = 25 and N = 150 for all measurements).

Discussion

Evidence from animal as well as human studies indicates that obesity and consumption of a Western diet may be associated with increased intestinal permeability [4,9,12,24]. One main consequence of increased intestinal permeability has been proposed to be the entry of endotoxins, such as LPS, from the intestinal lumen to the circulation [1,2]. A high blood endotoxin level can induce systemic inflammation through cytokine release and is considered a key event in the development of the chronic inflammatory state leading to insulin resistance in obesity [25,26]. High-fat and high-caloric diets have been shown to favor the colonization of the intestine with Gram-negative microbiota, leading to increased plasma levels of LPS [27].

The structure and function of the TJs appear to have a principal role in regulating paracellular transport across the intestinal epithelium, and barrier dysfunction is related to alterations in the expressions of TJ proteins [4,12,24]. The main core TJ units consist of the transmembrane proteins claudins and occludins and the scaffold protein zonula occludens. Although the core TJ units are composed of several different classes of proteins, which interact in a coordinated manner to form epithelial barriers, the claudins are clearly essential TJ proteins for the paracellular barrier properties [28,29]. There are however 2 subcategories of claudins: the pore forming claudins that increase the permeability through the formation of paracellular channels, such as claudin-2, and the claudins that generally have been associated with a more barrier tightening function, such as claudin-1, -3, -4 and -5 [29,30]. Decreased expression of these claudins has been described to increase the paracellular permeability [31]. It has been shown that probiotic bacteria can increase the expression of tightening TJ proteins, e.g., claudin-3, and improve barrier function [32] and prevent the development of colitis in neonate and adult rodents [33,34]. It was also shown that high-fat diet, not obesity per se was responsible for increased intestinal permeability specifically in the small, but not the large intestine of obese and lean rats. This was mediated by the suppressive effect of high-fat diet on the TJ proteins, including claudin-3 and occludin [35]. Probiotic components were able to partly prevent the detrimental effect of high-fat diet on uptake of LPS from the intestine by increasing TJ components e.g., claudin-3, -4, occludin and ZO-1 [36].

RYGB leads to a decrease of the chronic state of inflammation that is seen in obesity [16]. A normalized barrier function after RYGB may contribute to decreased inflammation and thereby improvement of obesity-associated metabolic complications. To our knowledge,

there are no reports on the effect of RYGB surgery on the expression of TJ proteins in small intestinal mucosa.

In our proteomics analysis of paired intraindividual jejunal mucosal samples before and 6–8 months after RYGB surgery, 1 of the main findings was an up-regulation of Ck8 protein. Ck8 has been shown to decrease intestinal permeability and possibly be of importance for the detoxification of LPS by intestinal alkaline phosphatase (ALP) in animal models [37,38].

Efficient cytokeratin proteins are required for an anatomically intact epithelium, and therefore our results suggested that the integrity of the small intestinal mucosa was changed after surgery. There are limitations to the sensitivity of the proteomics analysis, and we used relatively conservative criteria for the proteomics analysis. In this respect we decided to focus on the human intestinal barrier and therefore investigated levels of the paracellular permeability-regulating proteins of the TJs by Western blotting in additional paired intraindividual jejunal mucosal samples before and 6–8 months after RYGB surgery. The Western blot data confirmed the regulation of Ck8 from the proteomics analysis (Fig. 2), and showed presence of all investigated TJ proteins, and that claudins-3 and -4 were increased after RYGB surgery compared to baseline (Fig. 3). Because we did not have any normal weight controls, we do not know whether the baseline levels of the permeability related proteins were dysregulated in the obese patients. We did not find any group correlations between baseline characteristics, diabetes or gender on the baseline protein expression levels of TJ proteins.

Additional proteins are required to form functional TJ complexes. Most notable are the proteins zonula occludens and occludin that bind directly to the claudins and link them to the actin cytoskeletal network [29]. We observed decreased expression of both ZO-1 and occludin after RYGB surgery (Fig. 3). These results suggest a decreased attachment of the TJ links with the cytoskeleton, a condition known to compromise the sealing properties of the TJs [39]. The sealing properties of the TJs are strictly related to the expression and/or distribution of specific proteins. Whether the distribution is changed remains to be elucidated. The alimentary-limb, comprising a large proportion of the jejunum after the RYGB construction, is in addition to undigested nutrients, subjected to an increased microbial load, as the first protective barrier normally offered by the gastric acid is abolished by the surgical construction removing the major part of the ventricle from the passage of food.

Increasing evidence shows that the macroscopic appearance of the Roux-limb mucosa is changed after RYGB surgery. The histomorphometric findings in the present study displayed a substantial decrease in the villous surface area 6–8 months after RYGB surgery. Remodeling of the mucosa (e.g., by a flattened villous structure and increased cell proliferation) has been reported previously [19,40]. All

of these factors, including the decreased villous surface, that change the intraluminal environment may be factors explaining the down-regulations of occludin and ZO-1.

To assess which of the found TJ protein regulations that have predominant effect on the permeability of the intestinal mucosa, we used the Ussing chamber technique and the Ussing pulse method for assessment of the epithelial electrical resistance and transepithelial potential difference, a method that recently was validated against other permeability measurements [23]. We found that the intestinal epithelial electrical resistance (Rep) was correlated with claudin-3 expression in the corresponding mucosal samples, but not to Ck8 or claudin-4 (Fig. 4) or any of the other TJ proteins of the jejunal mucosa. This is an indication that claudin-3 is the predominant tight-junction protein regulating jejunal mucosal paracellular permeability. Thus, this suggests that jejunal mucosal permeability is decreased after RYGB surgery by decreased paracellular permeability caused by increased TJ function.

In summary, several alterations were found in the small intestinal mucosa before and after RYGB surgery that suggest an altered mucosal barrier function. The surface area of the jejunal epithelial mucosa was substantially decreased. The structural and TJ proteins Ck8, claudin-3 and claudin-4 proteins were up-regulated, whereas occludin and ZO-1 were down-regulated after RYGB surgery. Furthermore, when investigating the permeability of jejunal mucosal samples from obese patients in Ussing chamber experiments, we found a positive linear correlation between the epithelial electrical resistance and claudin-3 protein expression, but not with any of the other TJs. Taken together these results suggest that small intestinal permeability is decreased after RYGB. This could be an important event in the improvement of the metabolic state of the obese patients after RYGB, by decreasing the uptake of intestinal intraluminal bacterial components that are drivers of the chronic systemic inflammation and insulin resistance in obesity. Further research into the details of these mechanisms may open up for new future treatment regimens.

Disclosures

The authors have no commercial associations that might be a conflict of interest in relation to this article.

References

- [1] Carvalho BM, Saad MJ. Influence of gut microbiota on subclinical inflammation and insulin resistance. *Mediators Inflamm* 2013;2013: 986734.
- [2] Frazier TH, DiBaise JK, McClain CJ. Gut microbiota, intestinal permeability, obesity-induced inflammation, and liver injury. *JPEN J Parenter Enteral Nutr* 2011;35:14S–20S.
- [3] Turnbaugh PJ, Hamady M, Yatsunenko T, et al. A core gut microbiome in obese and lean twins. *Nature* 2009;457:480–4.
- [4] Brun P, Castagliuolo I, Di Leo V, et al. Increased intestinal permeability in obese mice: new evidence in the pathogenesis of

- nonalcoholic steatohepatitis. *Am J Physiol Gastrointest Liver Physiol* 2007;292:G518–25.
- [5] Siebler J, Galle PR, Weber MM. The gut-liver-axis: endotoxemia, inflammation, insulin resistance and NASH. *J Hepatol* 2008;48:1032–4.
- [6] Teixeira TF, Collado MC, Ferreira CL, Bressan J, Peluzio Mdo C. Potential mechanisms for the emerging link between obesity and increased intestinal permeability. *Nutr Res* 2012;32:637–47.
- [7] Ley RE, Turnbaugh PJ, Klein S, Gordon JI. Microbial ecology: human gut microbes associated with obesity. *Nature* 2006;444:1022–3.
- [8] Turnbaugh PJ, Ley RE, Mahowald MA, Magrini V, Mardis ER, Gordon JI. An obesity-associated gut microbiome with increased capacity for energy harvest. *Nature* 2006;444:1027–31.
- [9] Pendyala S, Walker JM, Holt PR. A high-fat diet is associated with endotoxemia that originates from the gut. *Gastroenterology* 2012;142:1100–1, e2.
- [10] Amar J, Burcelin R, Ruidavets JB, et al. Energy intake is associated with endotoxemia in apparently healthy men. *Am J Clin Nutr* 2008;87:1219–23.
- [11] Backhed F. Changes in intestinal microflora in obesity: cause or consequence? *J Pediatr Gastroenterol Nutr* 2009;48(Suppl 2):S56–7.
- [12] Cani PD, Neyrinck AM, Fava F, et al. Selective increases of bifidobacteria in gut microflora improve high-fat-diet-induced diabetes in mice through a mechanism associated with endotoxaemia. *Diabetologia* 2007;50:2374–83.
- [13] Shen L, Su L, Turner JR. Mechanisms and functional implications of intestinal barrier defects. *Dig Dis* 2009;27:443–9.
- [14] Sjostrom L. Review of the key results from the Swedish Obese Subjects (SOS) trial — a prospective controlled intervention study of bariatric surgery. *J Intern Med* 2013;273:219–34.
- [15] Carlsson LM, Peltonen M, Ahlin S, et al. Bariatric surgery and prevention of type 2 diabetes in Swedish obese subjects. *N Engl J Med* 2012;367:695–704.
- [16] Monte SV, Caruana JA, Ghanim H, et al. Reduction in endotoxemia, oxidative and inflammatory stress, and insulin resistance after Roux-en-Y gastric bypass surgery in patients with morbid obesity and type 2 diabetes mellitus. *Surgery* 2012;151:587–93.
- [17] Laurenius A, Larsson I, Melanson KJ, et al. Decreased energy density and changes in food selection following Roux-en-Y gastric bypass. *Eur J Clin Nutr* 2013;67:168–73.
- [18] le Roux CW, Bueter M, Theis N, et al. Gastric bypass reduces fat intake and preference. *Am J Physiol Regul Integr Comp Physiol* 2011;301:R1057–66.
- [19] Spak E, Bjorklund P, Helander HF, et al. Changes in the mucosa of the Roux-limb after gastric bypass surgery. *Histopathology* 2010;57:680–8.
- [20] Mayhew TM. The new stereological methods for interpreting functional morphology from slices and organs. *Exp Physiol* 1991;76:639–65.
- [21] Shevchenko A, Tomas H, Havlis J, Olsen JV, Mann M. In-gel digestion for mass spectrometric characterization of proteins and proteomes. *Nat Protoc* 2006;1:2856–60.
- [22] Bradford MM. A rapid and sensitive method for the quantitation of microgram quantities of protein utilizing the principle of protein-dye binding. *Anal Biochem* 1976;72:248–54.
- [23] Bjorkman E, Casselbrant A, Lundberg S, Fandriks L. In vitro assessment of epithelial electrical resistance in human esophageal and jejunal mucosae and in Caco-2 cell layers. *Scand J Gastroenterol* 2012;47:1321–33.
- [24] Cani PD, Bibiloni R, Knauf C, et al. Changes in gut microbiota control metabolic endotoxemia-induced inflammation in high-fat diet-induced obesity and diabetes in mice. *Diabetes* 2008;57:1470–81.
- [25] de Kort S, Keszthelyi D, Masclee AA. Leaky gut and diabetes mellitus: what is the link? *Obes Rev* 2011;12:449–58.
- [26] Diamant M, Blaak EE, de Vos WM. Do nutrient-gut-microbiota interactions play a role in human obesity, insulin resistance and type 2 diabetes? *Obes Rev* 2011;12:272–81.
- [27] Ley RE, Backhed F, Turnbaugh P, Lozupone CA, Knight RD, Gordon JI. Obesity alters gut microbial ecology. *Proc Natl Acad Sci U S A* 2005;102:11070–5.
- [28] Marchiando AM, Shen L, Graham WV, et al. The epithelial barrier is maintained by in vivo tight junction expansion during pathologic intestinal epithelial shedding. *Gastroenterology* 2011;140:1208–18, e1–2.
- [29] Overgaard CE, Daugherty BL, Mitchell LA, Koval M. Claudins: control of barrier function and regulation in response to oxidant stress. *Antioxid Redox Signal* 2011;15:1179–93.
- [30] Kotler BM, Kerstetter JE, Insogna KL. Claudins, dietary milk proteins, and intestinal barrier regulation. *Nutr Rev* 2013;71:60–5.
- [31] Amasheh S, Milatz S, Krug SM, et al. Tight junction proteins as channel formers and barrier builders. *Ann N Y Acad Sci* 2009;1165:211–9.
- [32] Patel RM, Myers LS, Kurundkar AR, Maheshwari A, Nusrat A, Lin PW. Probiotic bacteria induce maturation of intestinal claudin 3 expression and barrier function. *Am J Pathol* 2012;180:626–35.
- [33] Khailova L, Dvorak K, Arganbright KM, et al. Bifidobacterium bifidum improves intestinal integrity in a rat model of necrotizing enterocolitis. *Am J Physiol Gastrointest Liver Physiol* 2009;297:G940–9.
- [34] Mennigen R, Nolte K, Rijcken E, et al. Probiotic mixture VSL#3 protects the epithelial barrier by maintaining tight junction protein expression and preventing apoptosis in a murine model of colitis. *Am J Physiol Gastrointest Liver Physiol* 2009;296:G1140–9.
- [35] Suzuki T, Hara H. Dietary fat and bile juice, but not obesity, are responsible for the increase in small intestinal permeability induced through the suppression of tight junction protein expression in LETO and OLETF rats. *Nutr Metab (Lond)* 2010;7:19.
- [36] Neyrinck AM, Van Hee VF, Piront N, et al. Wheat-derived arabinoxylan oligosaccharides with prebiotic effect increase satiety-gut peptides and reduce metabolic endotoxemia in diet-induced obese mice. *Nutr Diabetes* 2012;2:e28.
- [37] Ameen NA, Figueroa Y, Salas PJ. Anomalous apical plasma membrane phenotype in CK8-deficient mice indicates a novel role for intermediate filaments in the polarization of simple epithelia. *J Cell Sci* 2001;114:563–75.
- [38] Wang L, Srinivasan S, Theiss AL, Merlin D, Sitaraman SV. Interleukin-6 induces keratin expression in intestinal epithelial cells: potential role of keratin-8 in interleukin-6-induced barrier function alterations. *J Biol Chem* 2007;282:8219–27.
- [39] Madara JL. Intestinal absorptive cell tight junctions are linked to cytoskeleton. *Am J Physiol* 1987;253:C171–5.
- [40] Saeidi N, Meoli L, Nestoridi E, et al. Reprogramming of intestinal glucose metabolism and glycemic control in rats after gastric bypass. *Science* 2013;341:406–10.